ELSEVIER

Biochimica et Biophysica Acta 1420 (1999) 189–202

BIOCHIMICA ET BIOPHYSICA ACTA
BBA

www.elsevier.com/locate/bba

New fluorescent cholesterol analogs as membrane probes

Irina V. Grechishnikova [a], Fredric Bergström [b], Lennart B.-Å. Johansson [b], Rhoderick E. Brown [c], Julian G. Molotkovsky [a,*]

[a] *Shemyakin and Ovchinnikov Institute of Bioorganic Chemistry, Russian Academy of Sciences, ul. Miklukho-Maklaya 16/10, Moscow 117871, Russian Federation*

[b] *Department of Physical Chemistry, Umeå University, S-901 87 Umeå, Sweden*

[c] *The Hormel Institute, University of Minnesota, Austin, MN 55912, USA*

Received 17 May 1999; accepted 2 June 1999

Abstract

New fluorescent cholesterol analogs, (22*E*,20*R*)-3β-hydroxy-23-(9-anthryl)-24-norchola-5,22-diene (*R*-AV-Ch), and the 20*S*-isomer (*S*-AV-Ch) were synthesized, their spectral and membrane properties were characterized. The probes bear a 9-anthrylvinyl (AV) group instead of C22–C27 segment of the cholesterol alkyl chain. Computer simulations show that both of the probes have bulkier tail regions than cholesterol and predict some perturbation in the packing of membranes, particularly for *R*-AV-Ch. In monolayer experiments, the force–area behavior of the probes was compared with that of cholesterol, pure and in mixtures with palmitoyloleoyl phosphatidylcholine (POPC) and *N*-stearoyl sphingomyelin (SSM). The results show that pure *R*-AV-Ch occupies 35–40% more cross-sectional area than cholesterol at surface pressures below film collapse (0–22 mN/m); whereas *S*-AV-Ch occupies nearly the same molecular area as cholesterol. Isotherms of POPC or SSM mixed with 0.1 mol fraction of either probe are similar to isotherms of the corresponding mixtures of POPC or SSM with cholesterol. The probes show typical AV absorption (λ 386, 368, 350 and 256 nm) and fluorescence (λ 412–435 nm) spectra. Steady-state anisotropies of *R*-AV-Ch and *S*-AV-Ch in isotropic medium or liquid–crystalline bilayers are higher than the values obtained for other AV probes reflecting hindered intramolecular mobility of the fluorophore and decreased overall rotational rate of the rigid cholesterol derivatives. This suggestion is confirmed by time-resolved fluorescence experiments which show also, in accordance with monolayer data, that *S*-AV-Ch is better accommodated in POPC–cholesterol bilayers than *R*-AV-Ch. Model and natural membranes can be labeled by either injecting the probes via a water-soluble organic solvent or by co-lyophilizing probe and phospholipid prior to vesicle production. Detergent-solubilization studies involving 'raft' lipids showed that *S*-AV-Ch almost identically mimicked the behavior of cholesterol and that of *R*-AV-Ch was only slightly inferior. Overall, the data suggest that the AV-labeled cholesterol analogs mimic cholesterol behavior in membrane systems and will be useful in related studies.

Keywords: Sterol analog; Fluorescence parameter; Anthrylvinyl; Monolayer; Model bilayer; Detergent-insolubility

Abbreviations: APC, 1-acyl-2-[12-(9-anthryl)-11*E*-dodecenoyl]-*sn*-glycero-3-phosphocholine; AV, 9-anthrylvinyl; *R*-AV-Ch, (22*E*,20*R*)-3β-hydroxy-23-(9-anthryl)-24-norchola-5,22-diene; *S*-AV-Ch, (22*E*,20*S*)-3β-hydroxy-23-(9-anthryl)-24-norchola-5,22-diene; DOPC, 1,2-dioleoyl-*sn*-glycero-3-phosphocholine; DPPC, 1,2-dipalmitoyl-*sn*-glycero-3-phosphocholine; NBD, 7-nitrobenz-2-oxa-1,3-diazol-4-yl; POPC, 1-palmitoyl-2-oleoyl-*sn*-glycero-3-phosphocholine; PSM, *N*-palmitoyl-sphingosine-1-phosphocholine; SSM, *N*-stearoyl-sphingosine-1-phosphocholine; T_m, main phase transition

* Corresponding author. Fax: +7-095-330-6601; E-mail: jgmol@ibch.siobc.ras.ru

0005-2736/99/$ – see front matter
PII: S0005-2736(99)00088-7

1. Introduction

Cholesterol is an important constituent in membranes of most eukaryotic cells where it may participate in the process of lipid domain formation in dynamic and structural ways. Its diverse and controversial role in membranes is a matter of numerous studies employing a wide variety of physical and chemical methods (for reviews, see [1–3]). Among the physical methods used to gain insight into cholesterol's role in membrane structure and function, fluorescence approaches have been useful despite a rather limited choice of sterol probes. Such probes include naturally fluorescent species as well as cholesterol derivatives with attached fluorescent reporter groups. Among the first group of sterols, dehydroergosterol and its analog cholesta-5,7,9(11)-trien-3β-ol are commonly used because of their close similarity, structurally and behaviorally in membranes, to natural cholesterol [4–7]. But the usefulness of these probes is limited especially with respect to fluorescence microscopy imaging applications because they have relatively low quantum yields, and they absorb in the UV region and emit in the UV and deep blue regions of the spectrum. Nevertheless, Mukherjee et al. recently used dehydroergosterol for fluorescence imaging microscopy of living cells. But this could be accomplished only by using sophisticated and specially designed equipment because many optical components of typical fluorescence microscopes absorb strongly in the UV region [8].

Among cholesterol analogs with attached reporter groups, derivatives with *N*-(7-nitrobenz-2-oxa-1,3-diazol-4-yl) (*N*-NBD) [9], 1-pyrenylmethoxycarbonyl [10] or 3-pyrenylamino [11] fluorophores in the side chain have been developed. However, because the lifetime of the NBD fluorophore depends on the medium polarity and pH in a complex way, and the lifetime of the pyrenyl excited state is quite long, these probes are not well suited to studies where fluorescence anisotropy is to be measured in membranes. Also, the increased polarity brought by these groups to the tail region of the molecule adversely affects the probes' properties relative to those of cholesterol. For example, the NBD-analog has shown quite a different pattern of distribution in cell membranes as compared to dehydroergosterol [8]. Cholesterol analogs with (*EEE*)-1-methyl-6-phenylhexatrien-1-yl and (*EE*)-1-methyl-4-(2-naphthyl)tetradien-1-yl fluorophores as a side chain also have been described [12], but little is known hitherto about their application. Other fluorescent sterols, more remotely related to native cholesterol, but similar to steroid hormones, are also available [13]. Each probe has its own merits as well as shortcomings.

It is clear that the cholesterol molecule is sensitive to the insertion of new groups that can change its properties drastically. For example, Gimpl and coworkers [14] have shown recently that substitution of cholesterol in the membrane environment of the oxytocin receptor by analogs containing polar groups in the sterol side chain strongly decreases binding efficiency of the receptor. Hence, careful design is a must for fluorescent probes intended to mimic cholesterol in membranes. It is critical to retain the 3β-OH interfacial anchor as well as the rigid 4-member ring system with angular methyl groups (see [8,15] for a discussion of this issue). It appears that the C17 side chain is the most suitable site for insertion of an external fluorophore. Previous work has shown that modifications of this part of the cholesterol molecule have the least negative impact on interaction with phospholipids in bilayer [16–18].

To avoid the disadvantages of earlier probes and to optimize the insertion point of the reporter group, we have prepared cholesterol analogs in which the apolar 9-anthrylvinyl (AV) group replaces part of the sterol side chain. Earlier we synthesized a series of AV-labeled phospholipid [19] and glycolipid [20] probes that showed a close similarity in membrane behavior as compared to their natural counterparts. Monolayer experiments have shown that low concentrations of AV-labeled phospholipids (up to 1 mol%) do not perturb lipid packing noticeably [19]. In addition, the AV fluorophore has several properties that are well-suited for membrane studies. These properties include good quantum yield and stability as well as convenient excitation and emission characteristics (see below). Also, the AV fluorophore can be useful in resonance energy transfer studies. The AV excitation spectrum overlaps the emission spectra of protein fluorophores (Tyr and Trp), a feature especially useful for studies of lipid–protein interactions. Moreover, the AV group can serve as an en-

ergy donor to other fluorophores, particularly 3-perylenoyl, making this pair suitable for studies of lipid–lipid interactions [19].

Based on the results of these earlier studies, we foresaw that attachment of the flat, non-polar AV group as part of the side chain of cholesterol would result in AV localization to the interior of the membrane. This localization would be expected to cause minor perturbation of the membrane, so that the probe actually can mimic natural cholesterol well. An interior bilayer localization of the fluorophore for phospholipids with AV in their acyl chains was demonstrated by ^{1}H-NMR investigations [19]. Based on these considerations, we have synthesized two AV-labeled analogs of cholesterol, *R*-AV-Ch and *S*-AV-Ch [21]. The probes have the AV group substituting for the C22–C27 tail of cholesterol and differ in configuration at C20 (Fig. 1). Here, we report on the basic photophysical properties of *R*-AV-Ch and *S*-AV-Ch, their characteristic behavior in model membrane systems, as well as describe potential applications of these new probes in membrane biophysical studies.

2. Materials and methods

2.1. Materials

Dioleoylphosphatidylcholine (DOPC), 1-palmitoyl-2-oleoylphosphatidylcholine (POPC), phosphatidylglycerol (EPG) derived from egg phosphatidylcholine, cholesterol and Tris were purchased from the Sigma Chemical Co; *N*-stearoyl sphingomyelin (SSM), its palmitoyl analog (PSM) [22], and AV-labeled PC (APC) [23] were prepared as described previously. The synthesis of the fluorescent cholesterol probes *R*-AV-Ch and *S*-AV-Ch [21] is summarized in Fig. 1.

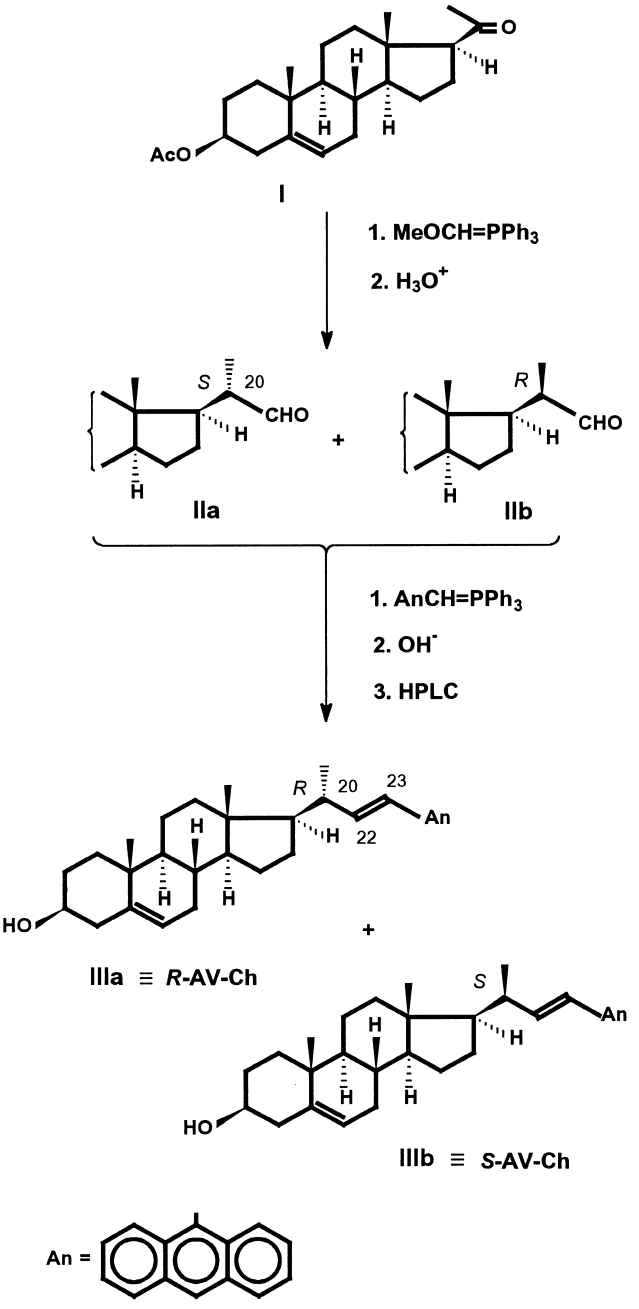

Fig. 1. Synthesis of *R*-AV-Ch and *S*-AV-Ch probes.

2.2. Computer simulations

The three-dimensional structures of cholesterol, *R*-AV-Ch and *S*-AV-Ch, were calculated based on energy minimization for isolated molecules in vacuo (Hyper Chem Molecular Modeling System program, version 3 for Windows; Hypercube). The calculations were performed by using the Excel 5.0 (Microsoft) and SURFER, Surface Mapping System (Golden Software, version 5.01) programs. The contour diagrams of steric energy reveal the existence of several minima for each molecule. Apart from the conformer structures corresponding to the lowest energy minimum (Fig. 2A), the structures (Fig. 2B) were chosen from the forms having their local energy min-

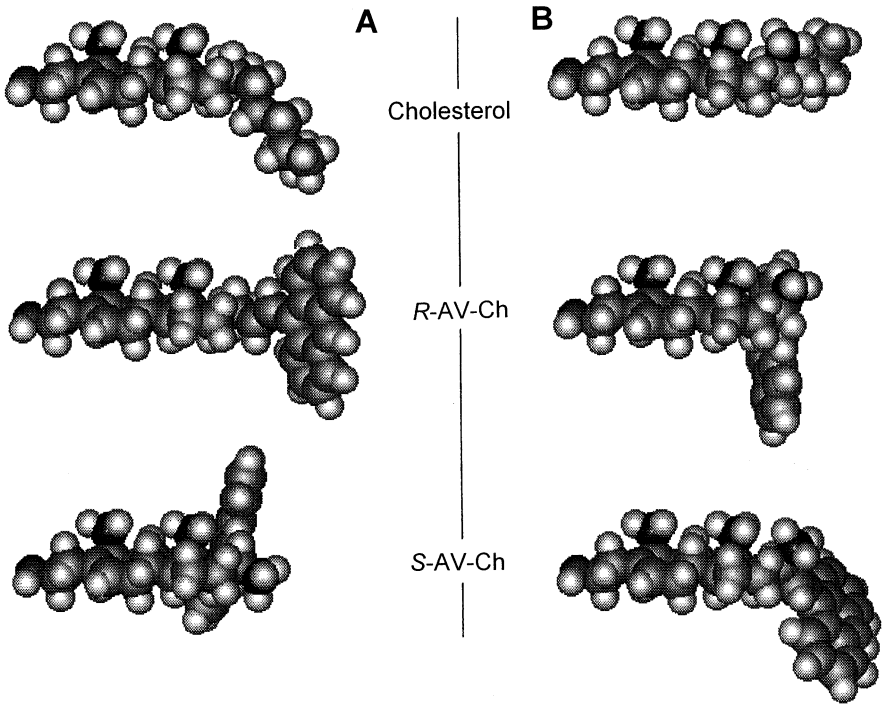

Fig. 2. Space-filling models. (A) Cholesterol, *R*-AV-Ch and *S*-AV-Ch at the lowest free energies. (B) Cholesterol, *R*-AV-Ch and *S*-AV-Ch at local free energy minima exceeding the lowest by ~4 kcal/mol and with 21-methyl group on the β-side of molecule. Hydroxy group is located on the left side of each molecule; 18-, 19- and 21-C atoms are shown in black.

ima and C21 methyl group located on the β-side of the molecule. Hence, these forms allow for a very similar and preferred conformation of the C21 methyl group, which has been proposed by Huang [24], Vanderkooi [25], and Robinson et al. [26].

2.3. Langmuir film balance measurements

Surface pressure versus molecular cross-sectional area isotherms were measured under a humidified argon atmosphere with a computer-controlled, Langmuir-type film balance calibrated according to the equilibrium spreading pressures of known lipid standards [27]. Lipids were dissolved (51.7 μl aliquots) and spread in hexane–ethanol (95:5). Films were compressed at a rate of <4 Å^2/molecule/min after an initial delay period of 4 min. The subphase temperature was maintained at fixed temperature with a thermostated, circulating water bath. Water for the subphase buffer was purified by reverse osmosis, activated charcoal adsorption, and mixed-bed deionization; then passed through a Milli-Q UV Plus System (Millipore, Bedford, MA); and filtered through a 0.22 μm Millipak 40 membrane. Subphase buffer (pH 6.6) consisting of 10 mM potassium phosphate, 100 mM NaCl, and 0.2% sodium azide was stored under argon until use. The monolayer isotherms were recorded at 24°C. Subphase buffer consisted of 10 mM potassium phosphate (pH 6.6), 100 mM NaCl, and 0.2% NaN_3 stored under argon until use.

2.4. Vesicle preparation and detergent-solubilization studies

An aliquot of lipid solution in chloroform was rotary-evaporated in a round-bottomed flask and kept in vacuo (20 Pa) for 2 h. The resulting thin lipid film was suspended in Tris-buffered saline (10 mM Tris-HCl in 150 mM NaCl, 1 mM EDTA, pH 7.4) lipid concentration 200 μg/ml, and kept for 40 min at 40°C on an ultrasonic bath cleaner under argon. Then, the lipid suspension was extruded through polycarbonate membranes (Nucleopore): 400 nm (5 times), 200 nm (5 times) and 100 nm (5 times). The vesicle size was determined by recording the 62.6° scattering of the 632.8 nm line of a helium–neon laser of a Coulter N4MD analyzer (Coultronics,

Margency, France). The mean vesicle diameter was found to be 130 ± 20 nm.

Two different approaches were used for probe insertion into membranes. In one approach, the *R*- or *S*-AV-Ch probe itself was dissolved in ethanol or dimethyl sulfoxide (0.2–0.5%), and then rapidly injected into a buffered suspension of cells or of bilayer extrusion vesicles composed of cholesterol and PC. The injected aliquot of AV-Ch was equivalent to about 1 mol% of the total lipid. Because the preceding approach resulted in incorporation of relatively minor amounts of AV-Ch into the membranes (see Section 3 for details), a second approach was used also. It involved co-dissolution of AV-Ch probes with DOPC (1:2–1:4) in organic solvent, evaporation of the solvent, resuspension of the dried lipids in ethanol, rapid injection of the dissolved lipids into stirring buffer, followed by extensive dialysis at 5–8°C [28]. Vesicles formed (50–100 μg/ml) were used within 6 h after preparation.

For Triton X-100 solubilization experiments, AV-Ch-containing vesicles were prepared by the protocol of Schroeder et al. [29]. Briefly, the dried lipid film was suspended in Tris-HCl buffer (20 mM, with 1 mM EDTA and 0.02% sodium azide, pH 7.4), bath sonicated for 1 h at 50°C under argon, and subjected to three freeze–thaw (15 min at 60°C) cycles to obtain opalescent suspensions (lipid concentration 200 μg/ml). Two ml of the vesicles were maintained 30 min at 4°C and 140 μl of refrigerated 10% Triton X-100 solution in the above buffer were added. After incubating for 20 min at 4°C, the mixture was centrifuged at 180 000 × *g* for 1.5 h at 4°C. Sedimented lipids and supernatant were recovered, separately suspended in 5 ml of buffer containing sodium dodecylsulfate (final concentration 2%), and bath sonicated (20 min at 40°C). Then AV-Ch probes were quantified by their fluorescence (see below).

Erythrocyte ghosts (unsealed) from human blood were prepared by the method of Shangguan et al. [30].

2.5. Spectral measurements

Steady-state fluorescence measurements were performed on a F-4000 fluorometer (Hitachi, Tokyo, Japan) or a SPEX Fluorolog 112 instrument by using thermostated 10 × 10 mm cuvettes with continuous stirring. The fluorescence spectra are corrected. The AV probes were excited at 370 or 389 (anisotropy measurements) nm and the emission was recorded at 430 nm (anisotropy measurements), with a 250–400-nm pass filter (Corning 9863) on excitation and a UV-39 filter (cut-off filter at wavelengths of < 390 nm) on emission to eliminate stray light. The spectral band width was 3 nm for excitation and 10 nm for emission. The UV spectra were recorded on a Ultrospec II spectrophotometer (Pharmacia LKB, Bromma, Sweden).

Time-correlated single photon measurements were performed on a PRA 3000 system (Photophysical Research, Ontario, Canada), using a thyratron-gated flash lamp (Model 510C, PRA) as excitation source. The lamp was filled with deuterium gas and operated at about 30 kHz. Interference filters (Omega/Saven, Sweden) centered at 389.9 nm (HBW = 10.0 nm) and 440 nm (HBW = 11.3 nm), were used to select the excitation and emission wavelengths, respectively. To avoid reabsorption, i.e. 'inner filter' effects, the maximum absorbance was kept below 0.08.

The fluorescence decay curves were measured by repeated collection of photons during 1000 s for each setting of the polarizers, $F_{vv}(t)$ and $F_{hv}(t)$. The subscripts vertical (v) and horizontal (h) indicate the orientations of the polarizers. A difference curve

$$D(t) = F_{vv}(t) - GF_{hv}(t)$$

and a sum curve

$$S(t) = F_{vv}(t) + 2GF_{hv}(t)$$

were constructed in every experiment. The scaling factor, G, was obtained by normalizing the total number of counts, F_{vv} and F_{hv}, to the steady-state anisotropy, r_s, according to

$$G = [(1 - r_s)F_{vv}]/[(1 + 2r_s)F_{hv}]$$

The time-resolved anisotropy was calculated from

$$r(t) = D(t)/S(t)$$

The fluorescence lifetimes were calculated by measuring decay curves with the excitation polarizer rotated 54.7° with respect to the emission polarizer. Deconvolution of the curves was performed on a Silicon Graphic Indy workstation (IRIS release 5.2) using a non-linear least squares analysis program,

based on a modified Levenberg–Marquardt algorithm [31–33].

3. Results and discussion

3.1. Cholesterol probe synthesis

The synthesis of the AV-labeled analogs of cholesterol, *R*-AV-Ch (**IIIa**) and *S*-AV-Ch (**IIIb**) is summarized in Fig. 1 and is described in detail earlier [21]. Briefly, 3β-acetoxy-5-pregnen-20-one (**I**) was subjected to a Wittig reaction with ylide from methoxymethyltriphenylphosphonium chloride, and subsequently hydrolyzed by an acid to give a 6:4 mixture (^{1}H-NMR and HPLC data) of epimeric 20*S*- (**IIa**) and 20*R*- (**IIb**) aldehydes. It should be noted that aldehyde **IIa**, which is 20*S* on the formal basis, has the same configuration as cholesterol which is 20*R*. It was shown earlier [34,35] that the Wittig olefination of the pregnenolone 20-keto group and subsequent hydrogenation of the resulting olefins led to the preferential formation of products with natural (20*R*) configuration irrespective to the olefin *E*- or *Z*-configuration. Without separation, the epimeric aldehydes **IIa** and **IIb** were reacted with 9-anthrylmethylenetriphenylphosphorane in another Wittig synthesis. Following alkaline hydrolysis to split off acetyl group, the *R*-AV-Ch (**IIIa**) and *S*-AV-Ch (**IIIb**) analogs were obtained accompanied by minor quantities of 20*R*,22*Z*- and 20*S*,22*Z*-isomers. The desired analogs **IIIa** and **IIIb** were purified by HPLC (a RP-18 column, mobile phase methanol–water, 19:1) and obtained with total yields of 40 and 21% correspondingly on the starting pregnenolone acetate **I**. The stereochemistry of **IIIa** and **IIIb** has been assigned based on their ^{1}H-NMR spectra. The more abundant 20*R*-isomer **IIIa** has chemical shift of 21-methyl group at a lower field ^{1}H-NMR peak (δ 1.37 ppm, $J_{21,20}$ 6.6 Hz) than 20*S*-compound **IIIb** (δ 1.33 ppm, $J_{21,20}$ 6.4 Hz); such interdependence has been shown previously on a series of related 20*R*- and 20*S*-compounds [34]. The 22*E*-structure of **IIIa** and **IIIb** follows from ^{1}H-NMR data (for H22: δ 5.88 ppm in **IIIa**, and 5.95 in **IIIb**, dd, $J_{22,23}$ 16.5 Hz; for H23: δ 7.05 in **IIIa**, and 7.09 in **IIIb**, d, $J_{23,22}$ 16.5 Hz) and fluorescence spectra (see below). It should be kept in mind that the probe with the same C20-configuration as in cholesterol is *R*-AV-Ch (**IIIa**), which originates from the 20*S*-aldehyde (**IIa**). From the *R*-aldehyde **IIb**, the *S*-AV-Ch probe **IIIb** was prepared.

3.2. Computer modeling

The 3-D structures of cholesterol and its AV analogs are shown in Fig. 2. Obviously, both *R*-AV-Ch and *S*-AV-Ch differ in their tail regions as compared to cholesterol. Note that, in the lowest energy conformations (Fig. 2A), the orientation of the AV fluorophore is nearly perpendicular to the plane of the tetracyclic ring system in a 'free-space' unrestricted environment for each of the fluorescent analogs. Yet, the bulky 'free space' conformations are not likely to occur in the anisotropic and somewhat restricted environment created by lipid acyl chains in bilayer or monolayer matrices. For this reason, we have considered the conformation of each probe at its local energy minima, with the C21 methyl group close to parallel with C18 and C19 methyls (see below). Under such conditions, no fully extended conformation for the AV ring relative to the tetracyclic sterol ring is obtained for *R*-AV-Ch. However, a conformer of *S*-AV-Ch, with energy only $\sim$4 kcal/mol higher than the lowest energy minimum, does show a relatively extended structure (Fig. 2B). In fact, as with a similar local-energy-minimum conformer of cholesterol, the energy minimized conformer of *S*-AV-Ch has the C21 methyl group located on β-side of the molecule. The almost parallel orientation of this group to C18 and C19 angular methyls should significantly stabilize the bilayer as it has been suggested earlier [24–26].

The model simulations suggest that, relative to cholesterol, both of the probes should produce some perturbation in the packing of membranes. The degree of perturbation is expected to be more pronounced for *R*-AV-Ch than for *S*-AV-Ch because the *R*-AV-Ch will maintain a bulkier, less-extended conformation in a lamellar environment. The situation can be rationalized for the following reasons: (1) the fluorophore is located at C20 and further away placing it close to the bilayer mid-plane region where acyl chain flexibility and degrees of freedom are greatest; (2) the fluorophore is not bound rigidly to the rest of molecule. A limited rotation about the

C17–C20 and C20–C22 bonds enhances accommodation by neighboring lipid molecules. Taken together, it would be predicted that perturbations in the membrane packing induced by *R*-AV-Ch or *S*-AV-Ch would be more pronounced at low values of surface pressure. This prediction is verified by monolayer experiments performed with a Langmuir-type film balance (see below).

3.3. Monolayer studies

To determine how well the modeling simulations predict the conformational behavior of *R*-AV-Ch and *S*-AV-Ch and how well these fluorophores mimic the behavior of native cholesterol, Langmuir film balance approaches were used to investigate the force–area behavior of the fluorescent sterol derivatives. The isotherms in Fig. 3 reveal several interesting features. First, the surface pressure versus average molecular area isotherms of *S*-AV-Ch (Fig. 3Cor D ; solid line) and of *R*-AV-Ch (Fig. 3E or F; solid line) show that both probes behave somewhat differently than native cholesterol (Fig. 3A or B; solid line). For instance, *R*-AV-Ch occupies 35–40% more cross-sectional area than cholesterol at equivalent surface pressures between 0 and 22 mN/m (e.g. Fig. 3E vs. A; solid line). Also, *R*-AV-Ch monolayers collapse at significantly lower pressures than cholesterol monolayers (22 vs. 45 mN/m). In contrast, *S*-AV-Ch occupies about the same cross-sectional molecular area as cholesterol at equivalent surface pressures between 0 and 23 mN/m. However, *S*-AV-Ch monolayers also collapse at significantly lower surface pressures than cholesterol monolayers (23 vs. 45 mN/m). Hence, with respect to interfacial behavior, it is clear that *S*-AV-Ch mimics native cholesterol better than *R*-AV-Ch. In this regard, the monolayer results support the conformational modeling simulations (see Section 3.2) which predict *R*-AV-Ch to be bulkier than *S*-AV-Ch.

To ascertain how well *R*-AV-Ch and *S*-AV-Ch mimic the mixing behavior of cholesterol with representative membrane lipids, the surface pressure versus average cross-sectional molecular area was determined when varying amounts of *R*-AV-Ch or *S*-AV-Ch (0.1-, 0.3-, 0.5-mol fractions) were mixed with POPC (Fig. 3E or C, respectively) or with SSM (Fig. 3F or D). For comparison, control experiments

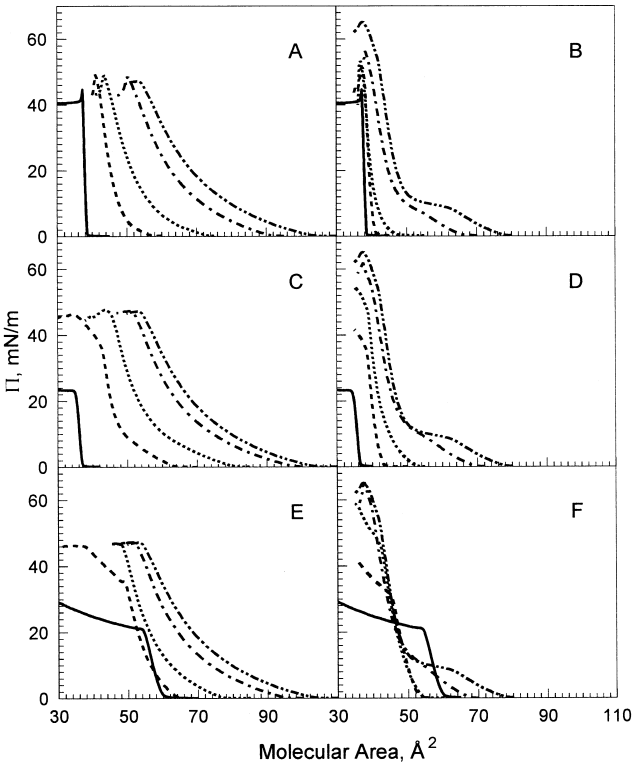

Fig. 3. Surface pressure versus average cross-sectional molecular area (Π–A). The monolayer isotherms were recorded at 24°C. The subphase buffer consisted of 10 mM potassium phosphate (pH 6.6), 100 mM NaCl, and 0.2% sodium azide; for other details see Section 2. (A) Cholesterol–POPC (mol/mol) isotherms. ———, pure cholesterol; - - -, cholesterol–POPC, 5:5; · · ·, cholesterol–POPC, 3:7; – · –, cholesterol–POPC, 1:9; - ·· -, pure POPC. (B) Cholesterol–SSM (mol/mol) isotherms. ———, pure cholesterol; - - -, cholesterol–SSM, 5:5; · · · cholesterol–SSM, 3:7; – · –, cholesterol–SSM, 1:9; - ·· -, pure SSM. (C) *S*-AV-Ch–POPC (mol/mol) isotherms. ———, pure *S*-AV-Ch–POPC; - - -, *S*-AV-Ch–POPC, 5:5; · · ·, *S*-AV-Ch–POPC, 3:7; – · –, *S*-AV-Ch–POPC, 1:9; - ·· -, pure POPC. (D) *S*-AV-Ch–SSM (mol/mol) isotherms. ———, pure *S*-AV-Ch–SSM; - - -, *S*-AV-Ch–SSM, 5:5; · · ·, *S*-AV-Ch–SSM, 3:7; – · –, *S*-AV-Ch–SSM, 1:9; - ·· -, pure SSM. (E) *R*-AV-Ch–POPC (mol/mol) isotherms. ———, pure *R*-AV-Ch–POPC; - - -, *R*-AV-Ch–POPC, 5:5; · · ·, *S*-AV-Ch–POPC, 3:7; – · –, *R*-AV-Ch–POPC, 1:9; - ·· -, pure POPC. (F) *R*-AV-Ch–SSM (mol/mol) isotherms. ———, pure *R*-AV-Ch–SSM; - - -, *R*-AV-Ch–SSM, 5:5; · · ·, *R*-AV-Ch–SSM, 3:7; – · –, *R*-AV-Ch–SSM, 1:9; - ·· -, pure SSM.

were performed with cholesterol–POPC mixtures (Fig. 3A) or with SSM (Fig. 3B). POPC was of particular interest because it is liquid–crystalline, i.e. liquid expanded, and has structural features regarded as being typical of membrane phosphoglycerides (e.g. saturated *sn*-1 and unsaturated *sn*-2 acyl chains). Isotherms of POPC mixed with 0.1-mol fraction *R*-AV-

Ch or *S*-AV-Ch (Fig. 3E and C, respectively) were almost identical to isotherms of POPC mixed with the same amount of cholesterol (Fig. 3A). With 0.3-mol fraction of the sterol derivatives, the *S*-AV-Ch films closely mimicked the behavior of cholesterol films at surface pressures above 10 mN/m; whereas *R*-AV-Ch films always had larger average molecular areas at equivalent surface pressures. A similar pattern was observed at 0.5-mol fraction sterol at surface pressures between 10 and 35 mN/m. However, a collapse or pre-collapse transition was evident near 37 mN/m for *S*-AV-Ch and near 35 mN/m for *R*-AV-Ch compared to 44 mN/m for films containing equimolar cholesterol.

In addition to comparing the mixing behavior of the *R*-AV-Ch and *S*-AV-Ch with cholesterol in POPC, experiments also were performed with SSM. This sphingomyelin species is a major component of bovine brain sphingomyelin. The two-dimensional phase transition of SSM is clearly evident in its isotherms (Fig. 3B, D, and F). This behavior has been reported previously: see e.g. [36], and references therein. As with cholesterol, mixing 0.1-mol fraction of either fluorescent sterol with SSM diminishes the sharpness of the 2-D phase transition. At 0.3-mol fraction sterol, the 2-D phase transition of SSM is completely eliminated regardless of sterol derivative. However, careful examination of the isotherms reveals that, at equivalent surface pressures, SSM films containing *S*-AV-Ch more closely imitate the area behavior of SSM–cholesterol. SSM films containing *R*-AV-Ch consistently have larger average molecular areas when compared at equivalent surface pressures below collapse at 0.3 and 0.5 sterol mol fraction. Particularly striking is the behavior of pure *R*-AV-Ch compared to *R*-AV-Ch-SSM mixtures (Fig. 3F). The results clearly show that mixing *R*-AV-Ch with SSM limits the probe's conformational behavior such that it occupies significantly less cross-sectional area than as a pure species. Nonetheless, even when mixed with SSM, *R*-AV-Ch is considerably more bulky than *S*-AV-Ch, which more closely mimics the interfacial behavior of cholesterol.

3.4. Light spectroscopic studies in liquid solutions and vesicles

The absorption and fluorescence spectra of both the probes *R*-AV-Ch and *S*-AV-Ch in ethanol are nearly identical, and characteristic for 9-anthrylvinyl system (cf. [23,37,38]); absorption: maxima at 386 (ε 7000), 368 (ε 7800), 350, and 256 nm (ε 1.3×10^5 M^{-1} cm^{-1}); fluorescence at 412–435 nm. This suggests that the fluorophore of both the probes has the same geometry as compared to other AV lipid derivatives. The polarity of the environment has only a minor influence on the AV fluorescence parameters [38]. Fig. 4 shows excitation and emission spectra of cholesterol analogs and phosphatidylcholine probe APC in the POPC vesicles.

The steady-state fluorescence anisotropy values of *R*-AV-Ch and *S*-AV-Ch in isotropic viscous medium, *rac*-2,3-butanediol, are 0.147 and 0.184 at 20°C. These values are higher than those obtained for other AV probes in the same environment (e.g. 0.094 for APC). The differences reflect hindered intramolecular mobility of the fluorophore as well as decreased overall rotational rate of the rigid cholesterol derivatives. It is noteworthy that *S*-AV-Ch has a higher anisotropy value than *R*-AV-Ch. This can be attributed to a higher stability of the conformation of the first probe realized in solution that makes mutual rota-

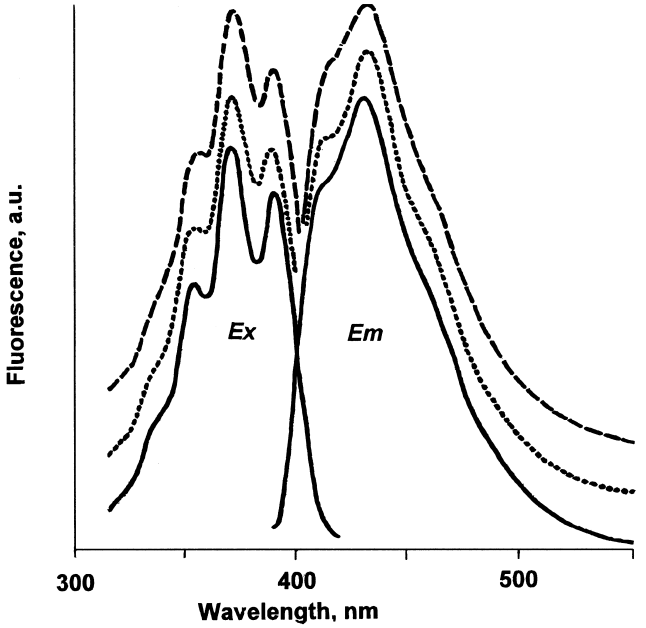

Fig. 4. Normalized excitation (emission, 432 nm) and emission (excitation, 370 nm) spectra of the probes: *R*-AV-Ch (———), *S*-AV-Ch (- - -) and APC (– – –) in POPC vesicles (200 μg/ml). Probe–lipid ratio, ~1:500; temperature, 20°C.

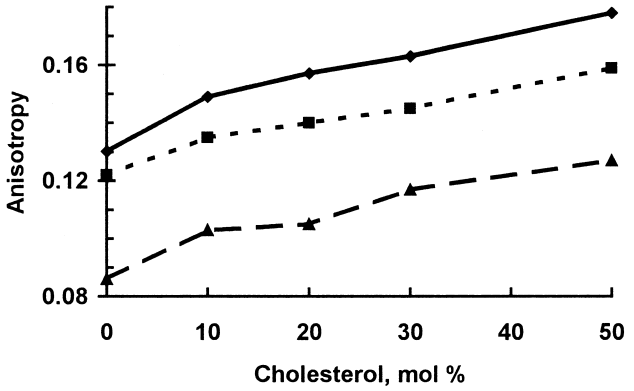

Fig. 5. Steady-state fluorescence anisotropy versus cholesterol content in POPC–cholesterol vesicles (200 μg/ml) of the probes: *R*-AV-Ch (———), *S*-AV-Ch (- - -) and APC (– – –). Probe–lipid ratio, ~1:500; temperature, 20°C.

tion of fluorophore and rest molecule less favorable than in the *R*-isomer.

In POPC vesicles containing various mole fractions of cholesterol (up to 0.5), the anisotropy increases upon increasing cholesterol concentration in the same way for both cholesterol analogs and APC (Fig. 5). Here, a higher anisotropy is obtained for *R*-AV-Ch as compared to *S*-AV-Ch, in the entire range of cholesterol concentrations. This situation is opposite to that in butanediol, but compatible with the presence of a lipid lateral pressure in the bilayer. Suppose that the OH group of cholesterol and of both probes is located at the same depth in the bilayer and close to the phospholipid ester carbonyl groups [25,39], then fluorophore of *S*-AV-Ch in its extended conformation (Fig. 2) can be localized closer to the middle of the bilayer than that of *R*-AV-Ch. This consideration is supported by rotational correlation time of the probes (see below). The anisotropy for three probes, *R*-AV-Ch and *S*-AV-Ch and APC, in POPC vesicles is temperature dependent and shows incremental decreases with increasing of temperature (Fig. 6). Since several parameters (i.e. the order parameter, the rotational correlation time(s), and the fluorescence lifetime) affect the steady-state anisotropy, no conclusive analysis of the data is possible without independent information.

It is known that, under certain conditions, anthracene derivatives may become 'stacked' or self-aligned within the bilayer environment. Tocanne and coworkers have studied this behavior using UV irradiation to generate non-fluorescent dimers among PC with *sn*-2 acyl chains carrying derivatized anthracenes (see [40] and references therein). Detailed analysis of the self-association process indicated a dynamic association–dissociation event that produces minimal interference with the photochemical properties of the probes because the lifetime of the excited state of the probe is much faster than its diffusional rate under fluid-phase conditions involving random probe distributions [41]. We noticed no tendency of our AV steroid fluorophores to stack under our membrane conditions, although such possibility exists under special circumstances, such as high probe concentrations, either total or local. We based this conclusion on the spectral responses obtained under other conditions where the total or local concentration of AV probe is high. Such a situation occurs with a 1.2 M solution of methyl (11*Z*)-12-(9-anthryl)-11-dodecenoate in isopropanol as well as with AV-labeled ganglioside GD1a in water which results in a micellar dispersion of the ganglioside. In both cases, the emission spectra contain an additional broad peak with a maximum at 470–490 nm and of low quantum yield which is associated with excimer formation among AV fluorophores [20]. No sign of excimer formation was observed in emission spectra of AV probes, either of cholesterol analogs or other, measured under conditions used in our membrane studies (e.g. probe concentrations 0.05–2 mol%).

For the three AV-derivatives solubilized in POPC vesicles containing different cholesterol contents, the fluorescence lifetimes are similar and about 11 ns, as

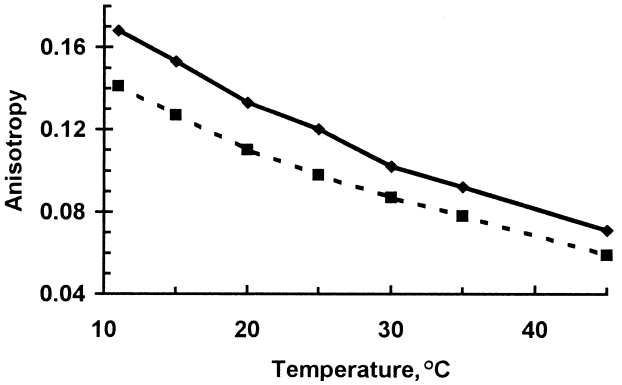

Fig. 6. Temperature dependence of steady-state fluorescence anisotropy in POPC vesicles (200 μg/ml) of the probes: *R*-AV-Ch (———) and *S*-AV-Ch (- - -). Probe–lipid ratio, ~1:500.

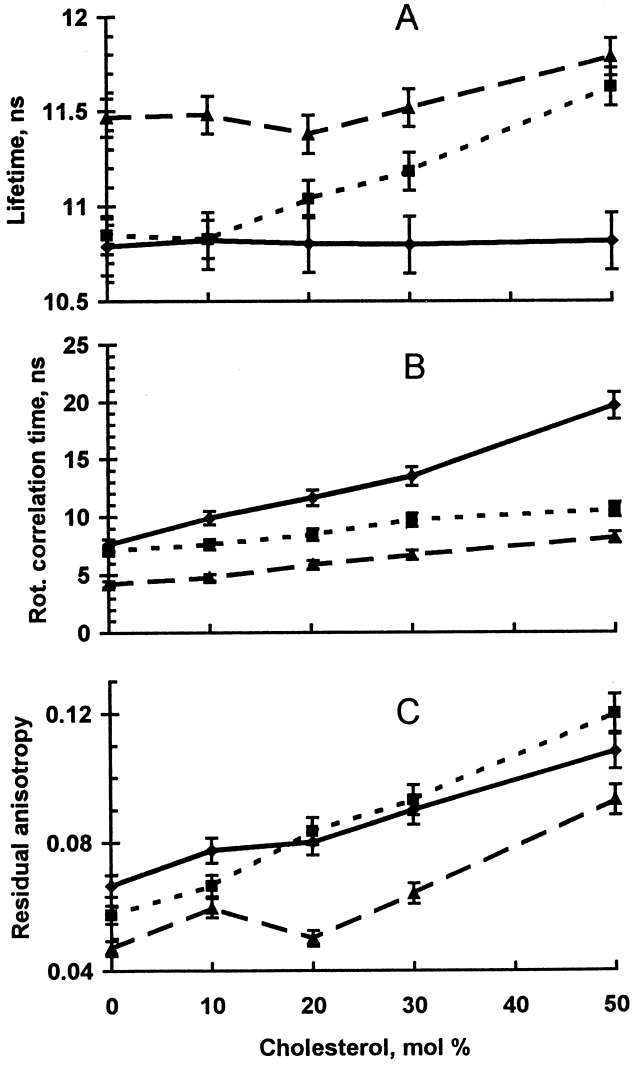

Fig. 7. Fluorescence lifetimes (A), rotation correlation times (B) and residual anisotropy (C) of *R*-AV-Ch (———), *S*-AV-Ch (- - -) and APC (– – –) in POPC vesicles with different cholesterol content. The lipid concentration was 1.07×10^{-2} M, the probe–lipid ratio was 1:1000, and temperature 14°C. The quality of fitting decay functions to the experimental data was judged by the statistical test parameters χ^2, Durbin–Wattson (DW) and weighted residuals. The values of χ^2 and DW were always less than 1.2 and larger than 1.7, respectively.

is shown in Fig. 7. The fluorescence relaxation of *R*-AV-Ch and *S*-AV-Ch is well described by a mono-exponential function, while the decays of APC are clearly bi-exponential, with a dominating lifetime of about 11.5 ns (>95%), and a shorter component of about 3 ns. For APC, the average lifetime is plotted in Fig. 7. The reason for a bi-exponential relaxation is not known. However, quite often fluorophores located in a microscopically anisotropic environment show more complex decays [33,42]. In the lipid layers studied here, the lifetime of *S*-AV-Ch increases while that for the *R*-form stays constant with increasing amounts of cholesterol. For APC, a rather weak dependence was also found. The different lifetimes can be explained by a varying O_2 concentration in the lipid bilayer, as well as by a cholesterol dependent rate of O_2 diffusion. Because the fluorophores are spatially distributed in the bilayer, the fluorescence quenching and thereby the lifetime is expected to vary.

The time-resolved fluorescence anisotropy experiments yield more details because they actually provide the orientational correlation function of the excited molecules. At all cholesterol concentrations, the fluorescence anisotropy decay, $r(t)$ could be fitted to the equation

$$r = (r_0 - r_\infty)\exp(-t/\phi) + r_\infty \quad (1)$$

In Eq. 1, r_0 and r_∞ denote the limiting and residual anisotropies, respectively. The rotational correlation time is ϕ. As could be seen from the Fig. 7B, the rotational rate decreases slightly for *S*-AV-Ch and APC, but is more pronounced for *R*-AV-Ch, with increasing cholesterol concentration in the lipid bilayer of POPC. The residual anisotropy or the order parameter increases with increasing cholesterol concentration for all AV derivatives, but the relative increase is strongest for *S*-AV-Ch and APC (Fig. 7C). The rather small change in rotational rate and the increase of order upon incorporating cholesterol is similar to other studies, see [43,44], and other works using as tools ESR and NMR spectroscopy [45,46]. The somewhat less relative increase in order of the *R*-AV-Ch suggests that this molecule does not pack as well as compared to the other probes. The latter is compatible with a less extended shape of the *R*-form as compared to the *S*-AV-Ch (Fig. 2) and agrees with the fluorescence steady-state anisotropy experiments (see above). Hence by increasing cholesterol concentration, the rotational motion of *R*-AV-Ch should become more hindered, with a stronger influence on the rotational correlation time (Fig. 7B). A packing in the lipid phase which is better adapted for the *S*-form, as compared to the *R*-AV-Ch, is also supported by monolayer experiments (see above).

Certainly, the anthrylvinyl group is a good deal bulkier than the $Me_2CH(CH_2)_3$ residue of cholesterol. Yet, localization to the most disordered region of the bilayer probably helps diminish the perturbation differences. Another possibility might be that the *S*-AV-Ch isomer disturbs the bilayer to a lesser extent because of its C20 *S*-configuration compared to the 20*R* configuration. But exactly how much influence such a change might have is unclear. Based on a somewhat analogous situation, the influence of the phospholipid *sn*-2 carbon chirality on interactions in membranes, remain controversial. An example is the function of gramicidin A and the related analog channel function which are not influenced by the phospholipid chirality [47]. However, Inagaki and co-workers [48] have reported conditions when phospholipid chirality does influence the two-dimensional structure of fluid lipid bilayers. Hence, the issue appears unsettled. Nonetheless, the data reported here suggest that the C20 configuration of *S*-AV-Ch should have little or no influence on the interactions of these probes with other molecules in membrane systems.

3.5. Incorporation of sterol probes into pre-formed bilayer vesicles and membranes

For model experiments, we introduced the AV analogs of cholesterol in a mixture of the matrix lipids. But labeling of pre-formed model preparations or natural membranes needs external addition of probes. We tested several procedures for labeling with the cholesterol probes of model membrane preparation, POPC–cholesterol (2:1, mol/mol) vesicles, and erythrocyte ghosts. It was concluded that the direct injection of a probe solution (0.2–0.5% in ethanol) in suspension of the POPC–cholesterol vesicles leads to a low degree of labeling. As judged from the fluorescence intensity, less than 15% of injected probes (0.2 mol % of total lipid) were inserted in the bilayer. In contrast to the phospholipid probe APC, a substantial part of the AV–cholesterol probe is absorbed in on glass walls of the incubation vessels in such experiments. The absorbed probe may be washed off by rinsing the walls with an appropriate solvent, e.g. a chloroform–methanol mixture. The extent of probe absorption to the vessel walls decreases when the ratio of wall area to probe quantity is reduced. A complete understanding of this phenomenon remains unclear, although this problem was encountered earlier by other authors, see e.g. [49].

More satisfactory results of model membrane labeling were obtained when AV–cholesterol analogs were added as components of mixed DOPC probe (2:1–4:1, mol/mol) vesicles. As much as 40% of the probe taken was included in model POPC–cholesterol (2:1) liposomes after 1-h incubation at 37°C. In the experiments on the labeling of natural membranes, both methods of the probe insertion gave similar results. Erythrocyte ghosts, after 1-h incubation at 37°C with *R*-AV-Ch or *S*-AV-Ch (ca. 0.5% of total lipid) added as 0.2% solution in dimethyl sulfoxide, incorporated from 5 to 15% of the probe. These values are several times lower than levels of incorporation in erythrocyte ghosts of AV-labeled phospholipids, e.g. APC under the same conditions (data not shown). Our preliminary experiments on the labeling of living culture of murine leukosis EL4 cells (not shown) also reveal that levels of insertion of cholesterol AV probes are several times lower than that of APC. Evidently, labeling of natural membranes and living cells with *R*-AV-Ch and *S*-AV-Ch probes is more complicated task than labeling with AV phospholipid probes, and will require additional studies.

3.6. Detergent solubilization of phospholipid-cholesterol vesicles ('raft' models)

One of the significant functions of cholesterol is its recently discovered ability to interact with sphingolipids to form specialized microdomains, or 'rafts', which are thought to play an important role in cellular signaling, adhesion etc. (for reviews see [50,51]). A characteristic feature of the 'rafts' is their resistance to solubilization by Triton X-100 at 4°C. Schroeder et al. [29] have shown in their model membrane experiments that liposomes consisting of cholesterol and high-melting, saturated chain phospholipids are resistant to cold Triton X-100 whereas liposomes with low-melting, unsaturated chain phospholipids are solubilized. It is thought that this resistance is brought about by interactions between acyl chains although hydrogen bonding may play a role [29].

We tested the abilities of *R*- and *S*-AV-Ch to render 'raft' lipids insoluble to Triton X-100. To accomplish this, we compared the solubilization of vesicles prepared from POPC–cholesterol, 4:1 ('solubizable') or from DPPC–PSM–cholesterol, 2:2:1 ('resistant') with vesicles in which either *R*-AV-Ch or *S*-AV-Ch was substituted for cholesterol. In control vesicles containing cholesterol, *R*-AV-Ch or *S*-AV-Ch was added as indicator (Table 1). In agreement with the previous studies of Schroeder et al. [29], our data show that the vesicles comprised of POPC ($T_m < 0$°C) are solubilized nearly entirely; whereas vesicles comprised of DPPC–BSM ($T_m > 40$°C for both) are resistant to detergent extraction. Analogous vesicles with AV-Ch probes substituting for cholesterol behave in a similar manner, although minor quantities of the probes appear to be extracted by Triton X-100. A subtle aspect of the data in Table 1 is the observation that the extent of the probe solubilization is always slightly higher for *R*-AV-Ch than for *S*-AV-Ch. This behavior is indicative of a slightly greater pertubation of lipid packing by *R*-AV-Ch compared to *S*-AV-Ch and is consistent with larger interfacial cross-sectional area predicted by the molecular modeling results and observed in the monolayer data (see Section 3.2 and 3.4). Nevertheless, the overall minor extent of the probes' solubilization closely resembles that of cholesterol in bilayers comprised of 'raft' lipids.

4. Conclusion

Earlier, we showed that AV-labeled phospho- and glycolipids are reliable investigative tools for membrane systems. These probes were used to study the molecular organization of human high-density lipoproteins [52], the interaction of prostaglandins with human low-density lipoproteins [53], the interaction of influenza virus with gangliosides [54], the activity of glycolipid transfer protein [55] and in others processes (for early works, see a review [19]). The data accumulated to date show that the AV group attached to the end of acyl chain produces minimal alterations in behavior of the probes as compared to unlabeled lipids.

At first glance, alterations might appear to be more significant when the AV group is introduced into cholesterol. But these alterations should not be overestimated because any structural change will impact to some degree. Even with dehydroergosterol, it should be noted that two of the additional double bonds significantly flatten the ring system as compared to that of cholesterol to say nothing of the additional double bond and methyl group in tail. Nevertheless, dehydroergosterol is now regarded as the best cholesterol-mimicking fluorescent probe [7,8] despite its UV excitation properties and low quantum yield. Our monolayer experiments show that AV-Ch probes, especially *S*-AV-Ch, at low concen-

Table 1
Triton X-100 solubilization of vesicles

Vesicle lipid composition, molar ratios[a]	Fluorescence (% of total)	
	Pellet	Supernatant
DPPC/BSM/*R*-AV-Ch, 40:40:20	89 ± 2	11 ± 2
DPPC/BSM/*S*-AV-Ch, 40:40:20	96 ± 2	4 ± 2
DPPC/BSM/Chol/*R*-AV-Ch, 40:40:19.5:0.5	93 ± 2	7 ± 2
DPPC/BSM/Chol/*S*-AV-Ch, 40:40:19.5:0.5	96 ± 2	4 ± 2
POPC/*R*-AV-Ch, 80:20[b]	3 ± 1	97 ± 1
POPC/*S*-AV-Ch, 80:20[b]	5 ± 1	95 ± 1
POPC/Chol/*R*-AV-Ch, 80:19.5:0.5[b]	4 ± 2	96 ± 2
POPC/Chol/*S*-AV-Ch, 80:19.5:0.5[b]	5 ± 2	95 ± 2

Vesicles were prepared by suspending the dried lipid film in Tris-HCl buffer, bath sonicating for 1 h at 50°C under argon, and subjecting to three freeze–thaw cycles. The final lipid concentration was 200 μg/ml. Two ml of the vesicles were maintained 30 min at 4°C prior to adding 140 μl of refrigerated 10% Triton X-100 solution in the above buffer. The mixture was incubated for 20 min at 4°C, and then centrifuged at 180 000 × *g* and 4°C for 1.5 h. Pelleted lipids and supernatant were separated and AV-Ch probes were quantified by their fluorescence.

[a] Chol, cholesterol.

[b] No sediment was observed.

trations produce minimal perturbations in the system packing. Moreover, the ability of the probes to modulate the detergent solubility of various lipid mixtures in a similar manner as cholesterol suggests that these probes will be quite useful.

Taken together, our data show that the AV-labeled cholesterol analogs, especially *S*-AV-Ch, are of potential interest for studies of the behavior of cholesterol in model and biological systems. These probes provide desirable fluorescent characteristics: convenient location of fluorescence maxima, high quantum yield and stability. Since AV fluorescence lifetime does not depend on the environmental polarity, measurements of the probes' anisotropy could be effective for monitoring of membrane fluidity in cholesterol-rich domains. The AV spectral characteristics also are favorable for studies of protein–cholesterol interactions via the resonance energy transfer technique. The same approach may be used for studies of cholesterol–lipid interactions because AV is a good donor for other fluorophores, such as the perylenoyl group [19]. Still, reasonable care should be observed in interpretation of results taking into consideration the actual differences of the probes and natural cholesterol. Additional studies are presently underway to further evaluate the usefulness of these sterol probes in studies of model and natural membranes.

Acknowledgements

We thank Dr. M.A. Sablina for help in performing of the computer simulation experiments, Dr. Howard Brockman for providing access to the Langmuir film balance, and Jan Smaby for monolayer technical assistance. We also gratefully acknowledge the support of a NAS/NRC COBASE Project Development Grant (J.G.M. and R.E.B.), the Swedish Natural Science Research Council (L.B.-Å.J.) and USPHS Grant GM45928 (R.E.B.). And we thank the anonymous Reviewers of the first version of our manuscript for their helpful insights and suggestions.

References

[1] P.L. Yeagle, in: L. Finegold (Ed.), Cholesterol in Membrane Models, CRC Press, Boca Raton, FL, 1993, pp. 1–12.
[2] M. Bloom, O.G. Mouritsen, in: R. Lipowsky, E. Sackmann (Eds.), Handbook of Biological Physics, Vol. 1, Elsevier Science, Amsterdam, 1995, pp. 65–95.
[3] T.P.W. McMullen, R.N. McElhaney, Curr. Opin. Colloid Interface Sci. 1 (1996) 83–90.
[4] J. Rogers, A.G. Lee, D.C. Wilton, Biochim. Biophys. Acta 552 (1979) 23–37.
[5] R.T. Fischer, F.A. Stephenson, A. Shafiee, F. Schroeder, J. Biol. Phys. 13 (1985) 13–24.
[6] R.T. Fischer, F.A. Stephenson, A. Shafiee, F. Schroeder, Chem. Phys. Lipids 36 (1984) 1–14.
[7] F. Schroeder, J.K. Woodford, J. Kavecansky, W.G. Wood, C. Joiner, Mol. Membr. Biol. 12 (1995) 113–119.
[8] S. Mukherjee, X. Zha, I. Tabas, F.R. Maxfield, Biophys. J. 75 (1998) 1915–1925.
[9] I.F. Craig, D.P. Via, W. Mantulin, N.J. Pownall, A.M. Gotto, L.C. Smith, J. Lipid Res. 22 (1981) 687–696.
[10] Y.J. Kao, M.C. Doody, L.C. Smith, J. Lipid Res 27 (1986) 781–785.
[11] Y.J. Kao, A.K. Soutar, K.Y. Hong, H.J. Pownall, L.C. Smith, Biochemistry 17 (1978) 2689–2696.
[12] J. Drew, M. Letellier, P. Morand, A.G. Szabo, J. Org. Chem. 52 (1987) 4047–4052.
[13] F. Schroeder, Prog. Lipid Res. 23 (1984) 97–113.
[14] G. Gimpl, K. Burger, F. Fahrenholz, Biochemistry 36 (1997) 10959–10974.
[15] R. Bittman, Subcellular Biochem. 28 (1997) 145–171.
[16] T. Nakamura, M. Nishikawa, K. Inoue, S. Nojima, T. Akiyama, U. Sankawa, Chem. Phys. Lipids 26 (1980) 101–110.
[17] M.A. Singer, L. Finegold, Chem. Phys. Lipids 56 (1990) 217–222.
[18] C. Vilcheze, T.P.W. McMullen, R.N. McElhaney, R. Bittman, Biochim. Biophys. Acta 1279 (1996) 235–242.
[19] L.D. Bergelson, J.G. Molotkovsky, Y.M. Manevich, Chem. Phys. Lipids 37 (1985) 165–195.
[20] J.G. Molotkovsky, I.I. Mikhalyov, A.B. Imbs, L.D. Bergelson, Chem. Phys. Lipids 58 (1991) 199–212.
[21] I.V. Grechishnikova, J.G. Molotkovsky, Bioorgan. Khim. 23 (1997) 422–427.
[22] J.M. Smaby, V.S. Kulkarni, M. Momsen, R.E. Brown, Biophys. J. 70 (1996) 868–877.
[23] J.G. Molotkovsky, P.I. Dmitriev, L.F. Nikulina, L.D. Bergelson, Bioorgan. Khim. 5 (1979) 588–594.
[24] C. Huang, Chem. Phys. Lipids 19 (1977) 150–158.
[25] G. Vanderkooi, Biophys. J. 66 (1994) 1457–1468.
[26] A.J. Robinson, W.G. Richards, P.J. Thomas, M.M. Hann, Biophys. J. 68 (1995) 164–170.
[27] W.E. Momsen, J.M. Smaby, H.L. Brockman, J. Colloid Interface Sci. 135 (1990) 547–552.
[28] R.E. Pagano, O.C. Martin, A.J. Schroit, D.K. Struck, Biochemistry 20 (1981) 4920–4927.
[29] R. Schroeder, E. London, D. Brown, Proc. Natl. Acad. Sci. USA 91 (1994) 12130–12134.
[30] T. Shangguan, C.C. Pak, S. Ali, A.S. Janoff, P. Meers, Biochim. Biophys. Acta 1368 (1998) 171–183.

[31] K. Levenberg, Quart. Appl. Math. 2 (1944) 164–168.
[32] D.W. Marquardt, J. Soc. Ind. Appl. Math. 11 (1963) 431–441.
[33] J. Karolin, M. Fa, M. Wilczynska, T. Ny, L.B.-Å. Johansson, Biophys. J. 74 (1998) 11–21.
[34] T.A. Narwid, K.E. Cooney, M.R. Uskokovic, Helv. Chim. Acta 57 (1974) 771–781.
[35] S.R. Schow, T.C. McMorris, J. Org. Chem. 44 (1979) 3760–3765.
[36] J.M. Smaby, M. Momsen, V.S. Kulkarni, R.E. Brown, Biochemistry 35 (1996) 5696–5704.
[37] M. Shinitzky, A.C. Dianoux, C. Gitler, G. Weber, Biochemistry 10 (1971) 2106–2113.
[38] L.B.-Å. Johansson, J.G. Molotkovsky, L.D. Bergelson, Chem. Phys. Lipids 53 (1990) 185–189.
[39] J. Villalain, Eur. J. Biochem. 241 (1996) 586–593.
[40] X. Ferriers, A. Lopez, A. Altibelli, L. Dupou-Cezanne, J.-L. Lagouanelle, J.-F. Tocanne, Biophys. J. 55 (1989) 1081–1091.
[41] F. Rodriguuez, J.-F. Tocanne, A. Lopez, Biophys. Chem. 53 (1995) 169–180.
[42] L.B.-Å. Johansson, J.G. Molotkovsky, L.D. Bergelson, J. Am. Chem. Soc. 109 (1987) 7374–7381.
[43] S. Kawato, K. Kinoshita Jr., A. Ikegami, Biochemistry 17 (1978) 5026–5031.
[44] M. Sassaroli, M. Ruonala, J. Virtanen, M. Vauhkonen, P. Somerharju, Biochemistry 34 (1995) 8843–8851.
[45] M. Pasenkiewicz-Gierula, W.K. Subczynski, A. Kusumi, Biochemistry 29 (1990) 4059–4069.
[46] J.L. Thewalt, M. Bloom, Biophys. J. 63 (1992) 1176–1181.
[47] L.L. Providence, O.S. Andersen, D.V. Greathouse, R.E. Koeppe, R. Bittman, Biochemistry 34 (1995) 16404–16411.
[48] M. Inagaki, M. Shibakami, S. Regen, J. Am. Chem. Soc. 119 (1997) 7161–7162.
[49] J.W. Nichols, Biochemistry 24 (1985) 6390–6398.
[50] R.E. Brown, J. Cell Sci. 111 (1998) 1–9.
[51] T. Harder, P. Scheiffele, P. Verkade, K. Simons, J. Cell Biol. 141 (1998) 929–942.
[52] J.G. Molotkovsky, Y.M. Manevich, E.N. Gerasimova, I.M. Molotkovskaya, V.A. Polessky, L.D. Bergelson, Eur. J. Biochem. 122 (1982) 573–579.
[53] Y.M. Manevich, M.A. Martynova, G.I. Muzya, E.L. Vodovozova, J.G. Molotkovsky, L.D. Bergelson, Biochim. Biophys. Acta 963 (1988) 302–310.
[54] V.A. Slepushkin, A.I. Starov, A.G. Bukrinskaya, A.B. Imbs, M.A. Martynova, L.S. Kogtev, E.L. Vodovozova, N.G. Timofeeva, J.G. Molotkovsky, L.D. Bergelson, Eur. J. Biochem. 173 (1988) 599–605.
[55] P. Mattjus, J.G. Molotkovsky, J.M. Smaby, R.E. Brown, Analyt. Biochem. 268 (1999) 297–304.